

# A COMPACT 335 MeV POSITRON DAMPING RING DESIGN FOR FACET-II\*

G. R. White<sup>†</sup>, Y. Cai, R. Hettel, M. Johansson, V. Yakimenko, G. Yocky,  
SLAC National Accelerator Laboratory, 2575 Sand Hill Road, Menlo Park, CA 94025, USA

## Abstract

FACET-II will be a new test facility, starting construction in 2018 within the main SLAC Linac. Its purpose is to build on the decades-long experience developed conducting accelerator R&D at SLAC in the areas of advanced acceleration and coherent radiation techniques with high-energy electron and positron beams. The positron system design utilizes an existing W-Re target in Linac Sector 19, driven by 4 nC electrons bunches at 10 GeV. We present the design of a 335 MeV, 21.4 m circumference damping ring required to damp emittance from a modified positron return beamline by a factor of 500. The transverse emittance is calculated to be 6  $\mu\text{m-rad}$ , fully coupled, with a bunch length of 4 mm and energy spread 0.06 %, at a bunch charge of 1 nC. The arc magnets need to be especially compact due to tight space constraints (installation will be in the existing SLAC Linac tunnel, Sector 10, with 3 m width available) and were a key design challenge. We present a solution with combined function bend/quadrupole/sextupole magnets which have been modelled in 3D using Opera.

## FACET-II POSITRON SYSTEM

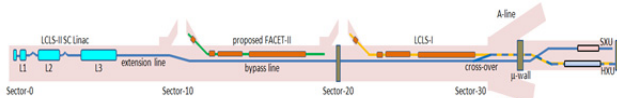


Figure 1: Location of FACET-II in SLAC Linac.

The goal in designing the FACET-II accelerator facility is to enable the delivery of high peak-current (10's kA), low emittance ( $< 20 \mu\text{m-rad}$  transverse, normalized) electron and positron bunches to users in the Sector 20 experimental region of the SLAC Linac.

FACET-II positron (and electron) systems will exist in the central 1 km region between Sectors 10 and 20 of the existing SLAC Linac (between the LCLS-II and existing LCLS accelerators) as shown in Fig. 1.

The positrons are generated by the existing FACET W-Re rotating target in Sector 19, fed by a 4 nC electron bunch generated by a new electron photo-cathode RF injector in Sector 10, and accelerated to 10 GeV in the common electron/positron accelerating sectors 11-19.

Positrons are returned to Sector 10 via the existing positron return line on the Linac ceiling. Four 7' s-band accelerating structures are added in Sector 14 of the return line to boost the 200 MeV positron energy to the 335 MeV required by the ring.

The positrons are vertically injected into the damping

ring in an on-axis injection scheme using a new septum magnet and re-using an existing SLC damping ring kicker.

After damping, the positrons are extracted vertically in a system mirroring the injection system. The beam is then pre-compressed to match the electron beam at this energy (from 4mm to 0.24 mm) and injected into the main Linac in the last bend of the first electron compressor chicane.

More details of the design of the FACET-II positron system (and of the rest of the FACET-II facility) can be found in the FACET-II technical design report [1].

## POSITRON DAMPING RING

Table 1: Main Parameters of the Positron Damping Ring Including IBS Calculations

Parameter	Value
Energy, $E$ [MeV]	335.0
Bunch Charge, $Q$ [nC]	1.0
Beam Current, $I$ [mA]	14.0
Circumference, $C$ [m]	21.41
RF Energy Acceptance, $A$ [%]	2.9
Tune, $\nu_a, \nu_b$	4.58, 2.58
Emittance, $\gamma\epsilon_{a,b}$ [ $\mu\text{m-rad}$ ]	5.5
Bunch length, $\sigma_z$ [mm]	3.9
Energy spread, $\sigma_\delta$ [%]	0.062
Momentum compaction, $\alpha_p$	0.0518
Damping partition, $J_x, J_y, J_z$	2.15, 1.0, 0.85
Damping time, $\tau_a, \tau_b, \tau_c$ [ms]	16.9, 36.4, 43.0
Natural Chromaticity, $\xi_{a0}, \xi_{b0}$	-6.5, -4.4
Chromaticity, $\xi_a, \xi_b$	+1, +1
Synchrotron Energy loss per turn, $U_0$ [keV]	1.362
RF voltage, $V_{RF}$ [MV]	1.1
RF frequency, $f_{RF}$ [MHz]	714.0
Harmonic Number [n]	51
Synchrotron Tune	0.037 (521.9 kHz, 26.8 turns)

As the positron beam emerges from the target and reaches an energy of 335 MeV, it has a normalized transverse emittance of 2 mm-rad in the horizontal and vertical planes. This emittance is 500X larger than the electron beam out of the photo-injector. A damping ring is necessary to reduce the positron x and y emittance values to the  $\mu\text{m-rad}$  level in a few milliseconds. User requirements are typically for a  $\sim 1$  Hz source of positron bunches (we expect to be able to operate at up to 5 Hz given the longitudinal damping time of  $\sim 40$  ms). The ring is placed in Sector 10, inside the existing Linac tunnel. This implies

\* Work supported by the Department of Energy under Contract Number: DE-AC02-76SF00515.

<sup>†</sup> whitegr@slac.stanford.edu

that the diameter of the ring must be smaller than 3 meters. This constraint dictates a compact design with minimal gaps between the magnets in the arcs.

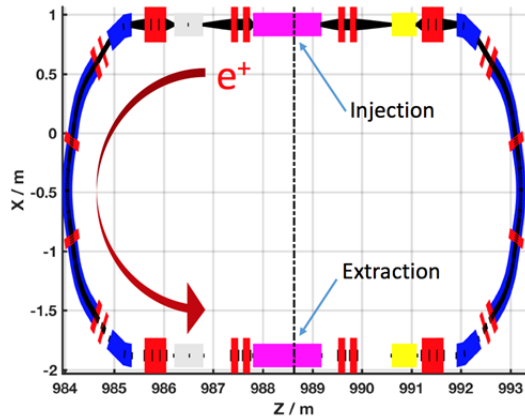


Figure 2: Positron damping ring. Combined-function bends are shown in blue, quadrupoles (combined function quad/sextupoles in arcs) are shown in red, septum magnets are magenta, kickers are grey and RF cavities are shown in yellow.

The ring is fully transversely coupled, achieved by operating on the integer tune resonance  $\nu_x - \nu_y = 2$ , with coupling controlled via excitations ( $\sim 1\%$  coupling parameter needed) of skew quads available in the straight sections. Coupling reduces the impact of IBS whilst permitting small longitudinal emittance. Also, the experimental program strongly benefits from positron beam with equal emittances.

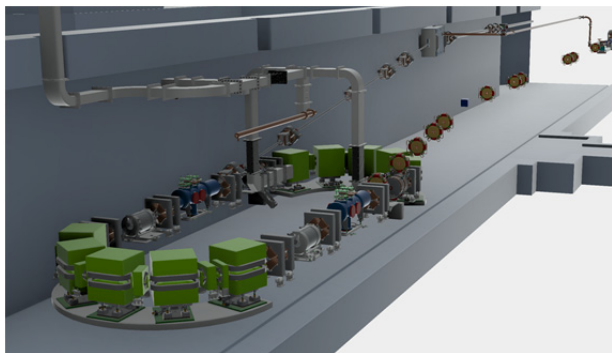


Figure 3: CAD model of positron damping ring for FACET-II located in the Sector 10 Linac tunnel. Injection line on the left side and the extraction beamline on the right side of the drawing (vacuum chamber not shown).

The fractional tunes are a result of the phase advances required for emittance and due to the constraints imposed by the required magnetic field strengths. Although above half integer tunes are not preferred from a point of view of instability driven by resistive-wall impedance, calculations show that the growth rate is much slower than the radiation damping rate. Moreover, ring designs with fractional tunes above a half integer were successfully used at PEP-II and KEKB.

Final transverse and longitudinal phase space is strongly impacted by IBS as shown in Fig. 7, the results of which are reflected in the parameters in Table 1.

The layout of the ring is shown schematically in Fig. 2, with a CAD model showing the ring installed into the main Linac tunnel in Sector 10 shown in Fig. 3.

Optics

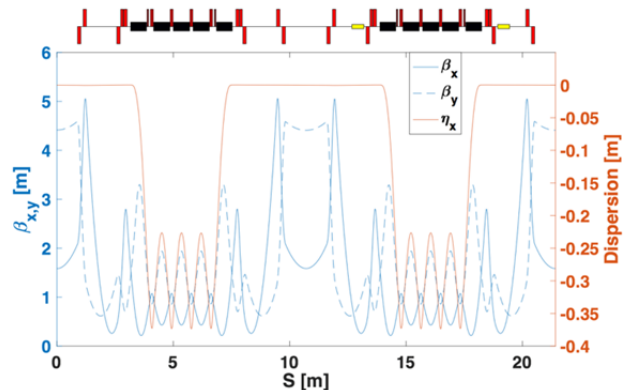


Figure 4: Lattice functions of the positron damping ring in FACET-II.

Three FB-cells using combined function dipole magnets with a defocusing gradient are used in the arcs. This lowers the horizontal beta functions and dispersion inside the dipole to minimize the emittance.

The dispersion in the arc is reduced to zero by a dispersion suppressor as the beam enters the straight. The straight sections contain the injection and extraction systems. Since they are dispersion free, they are also good regions in which to place RF cavities. The injection and extraction are vertical because of the limitation in the horizontal tunnel size. The optics that meets these requirements is shown in Fig. 4.

All arc magnets are combined-function, with the arc cells containing bend, quadrupole and sextupole fields. Due to the complex nature of the field structure of the arc magnets, a sliced model is used in the optics and beam dynamics modeling codes (BMAD [2] and AT [3]). The sliced model is tuned based on direct 3D particle tracking of the Opera [4] generated 3D field maps with the code GPT [5].

MAGNET DESIGN

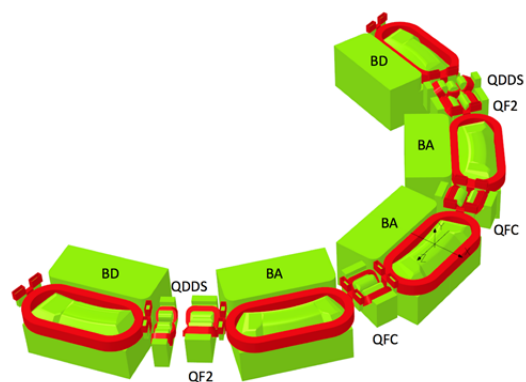


Figure 5: Magnets in the damping ring arcs.

The straight section of the ring contains conventional and single-function magnets only, consisting of focusing and defocusing quadrupoles and skew quadrupoles to control coupling. Adequate space is reserved for RF cavities, kickers and septa. The arc magnets consist of three combined function bend-quadrupole-sextupole magnets (labeled “BA”) and 2 combined function bend-quadrupole “dispersion suppressor” bends (“BD”). Between these are 3 families of combined function quadrupole-sextupole magnets (“QDD”, “QF2” and “QFC”). QF2 and QFC are quadrupole magnets with offset pole shapes to achieve the required sextupole components, the QDD magnets are designed as offset sextupole magnets.

The 3D layout from Opera of the arc magnets are shown in Fig. 5 with a close-up shown in Fig. 6 which demonstrates the compactness of the design. Note the field-clamps used to prevent field leakage between magnets. These also contain steering corrector windings which perform the function of orbit correction.

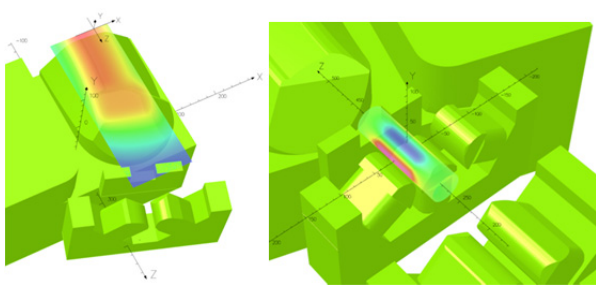


Figure 6: Details of 3D magnet designs for BA and QF2 magnets showing slices of 3D B field maps.

## BEAM DYNAMICS

The chromaticities and non-linear tune-shifts of the ring were evaluated using particle tracking with AT: the non-linear tune shifts are very modest, largely because of not much accumulation in the small ring. This analysis shows that the beam footprint in tune space should be small, avoiding nonlinear resonances.

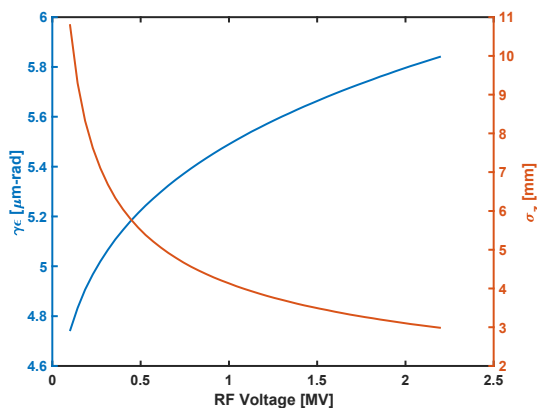


Figure 7: Normalized transverse emittance & bunch length parameters as a function of total RF voltage.

To calculate transverse emittance, bunch length and energy spread parameters, an IBS simulation implemented within the BMAD software suite is used. The simulation uses Bjorken & Mtingwa’s formula [6]. In principal, the ring has space to use up to four 714 MHz RF cavities, allowing up to 2.2 MV total RF ring voltage. Figure 7 shows the trade-off between transverse and longitudinal emittance depending on choice of RF voltage. Both need to be considered when considering the desired final positron bunch parameters in Sector 20.

A direct calculation of the dynamic aperture using the PTC [7] tracking model (from within BMAD) was performed and shown in Fig. 8. Particles are tracked for  $\sim 20\%$  of a damping period (100k turns) and the aperture presented up to the maximum  $\delta_E$  acceptance of the ring of 2.8%. The dynamic aperture of the ring appears to be sufficient to inject particles across the full physical aperture and up to the full RF energy acceptance at an RF voltage of 1.1 MV.

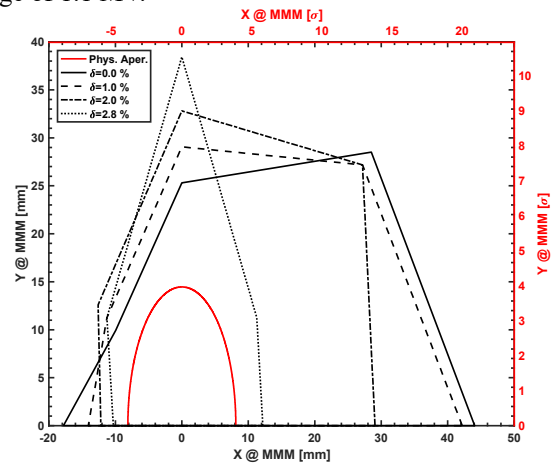


Figure 8: Dynamic aperture of the ring specified at the injection point & compared with the physical acceptance.

Potential sources of beam instabilities have been studied considering multiple sources: (i) the single-bunch microwave instability driven by CSR, (ii) the single-bunch transverse mode coupling instability (TMCI) due to the resistance in the walls, (iii) the multi-turn transverse instability driven by the wall resistance and (iv) the electron cloud instability. We find there to be no onset of collective instability at our design bunch charge of 1 nC.

## ACKNOWLEDGEMENTS

The authors would like to acknowledge the invaluable contribution to the design of the damping ring from the SLAC engineering groups; special thanks go to E. Bong and G. Bouchard.

**REFERENCES**

- [1] FACET-II Technical Design Report, SLAC-R-1072.
- [2] <https://www.classe.cornell.edu/~dcs/bmad/overview.html>, D. Sagan, “Design and Applications of the Bmad Library for the Simulation of Particle Beams and X-Rays”, ICAP2012, Rostock-Warnemunde, Germany (2012).
- [3] Accelerator Toolbox Collaboration, <http://atcollab.sourceforge.net>
- [4] Opera 18R2 (Build 36450) x64 Professional Edition, <http://operafea.com>
- [5] Pulsar Physics, <http://www.pulsar.nl/gpt>
- [6] Bjorken, J., Mtingwa, S., “Intrabeam Scattering”, Particle Accelerators. 13. Pp. 115-143 (1983).
- [7] É. Forest, Beam Dynamics: A New Attitude and Framework, Harwood Academic Publishers, Amsterdam (1998).